

Microwave Radiation from a High-Gain Free-Electron Laser Amplifier

T. J. Orzechowski, B. Anderson, W. M. Fawley, D. Prosnitz, E. T. Scharlemann, and S. Yarema
Lawrence Livermore National Laboratory, Livermore, California 94550

and

D. Hopkins, A. C. Paul, A. M. Sessler, and J. Wurtele
Lawrence Berkeley Laboratory, Berkeley, California 94720
(Received 1 October 1984)

A high-gain, high-extraction-efficiency, linearly polarized free-electron laser amplifier has been operated at 34.6 GHz. At low signal levels, exponential gain of 13.4 dB/m has been measured. With a 30-kW input signal, saturation was observed with an 80-MW output and a 5% extraction efficiency. The results are in good agreement with linear models at small signal levels and nonlinear models at large signal levels.

PACS numbers 42.60.By, 41.70.+t, 42.52.+x

The free-electron laser (FEL) is capable of producing coherent radiation from the ultraviolet to the microwave region of the electromagnetic spectrum. Several recent experiments have demonstrated low-gain, low-efficiency FEL operation in the visible¹ and infrared² regions while other experiments have demonstrated high-gain FEL operation in the millimeter-wave regime.^{3,4} We have designed an experiment, the Electron Laser Facility (ELF), which can serve as a test of the physical models used to predict high-gain and high-efficiency FEL operation in the visible spectral region. The ELF consists of an amplifier with well-defined initial conditions on the radiation and the electron beam and with no axial magnetic field.

Figure 1 shows the experimental configuration used in the ELF.⁵ We utilized the Lawrence Livermore National Laboratory experimental test accelerator⁶ to provide a 6-kA, ~ 3.3 -MeV beam with a normalized emittance of 1.5π rad cm. An emittance filter is used to reduce the beam current to approximately 500 A (pulse length of 15 ns) with a normalized edge emittance⁷ of 0.47π rad cm.

The 3-m-long wiggler is composed of specially shaped solenoids to provide a linearly polarized wiggler with a 9.8-cm period. The pulsed wiggler can provide a peak field on axis of 5 kG. Each two periods of the wiggler is energized by a separate power supply which allows variation of the strength and longitudinal profile of the wiggler field, although the experiments described here use a constant-amplitude wiggler. Vertical focusing of the electron beam is provided by the natural focusing of the wiggler field. Horizontal focusing is achieved with continuous quadrupoles with a field gradient of 30 G/cm. The magnets surround a 2.9×9.8 -cm² stainless-steel waveguide which serves as the interaction region.

The microwave input to the amplifier was provided by a 34.6-GHz, 60-kW pulsed magnetron (pulse length of 500 ns). This input signal was injected into the

TE₀₁ mode of the interaction region by means of waveguide tapers (to match smoothly the WR28 output waveguide of the magnetron to the oversized FEL waveguide) and a fine wire mesh reflector (see Fig. 1). The electron beam passed through this mesh with no loss of current and negligible emittance growth. Measurements showed that conversion from the TE₁₀ mode of the fundamental guide to the TE₀₁ mode of the oversized guide resulted in a 3-dB loss of input sig-

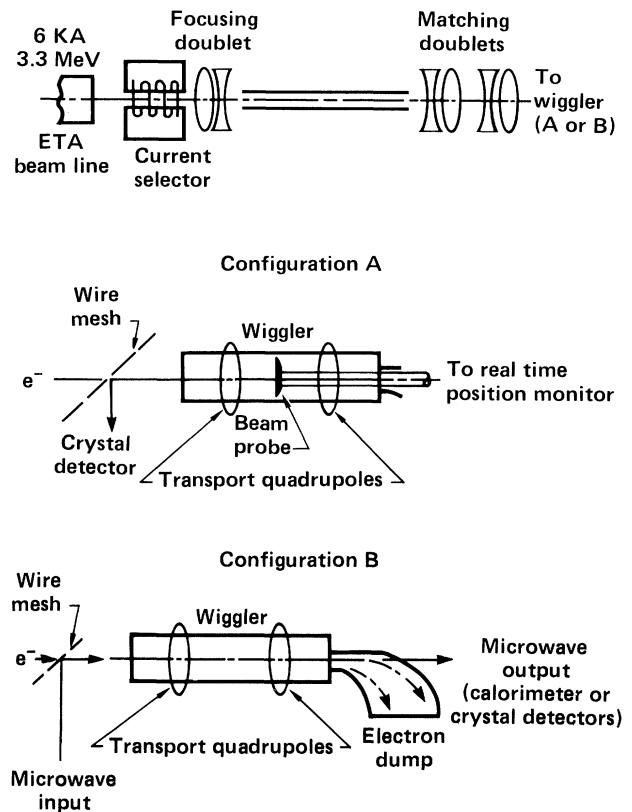


FIG. 1. Experimental configuration.

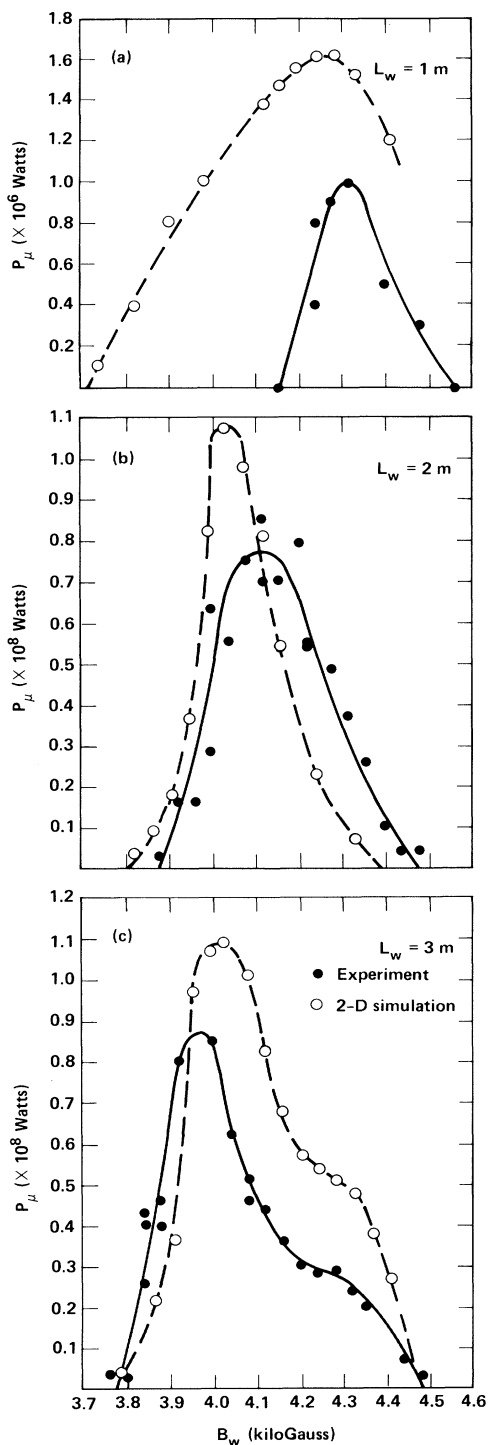


FIG. 3. Microwave power output as a function of wiggler magnetic field for various wiggler lengths.

tion while obeying the γ - ψ equations.⁸ The longitudinal equations in the simulation use local values of the fields; thus off-axis effects are fully modeled including

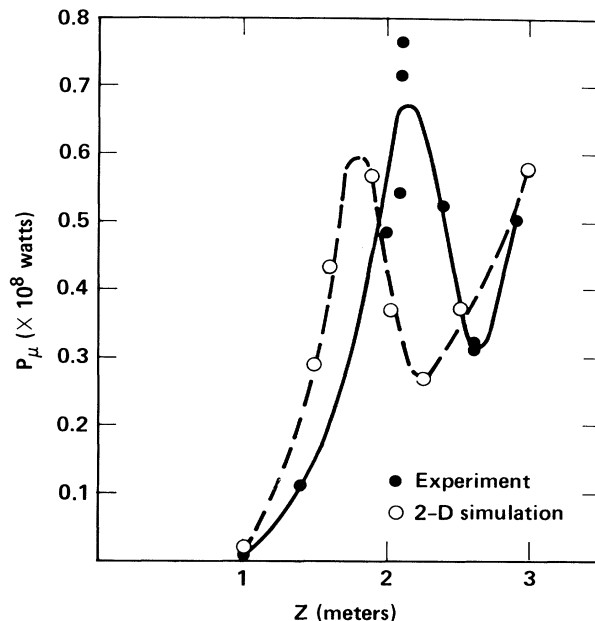


FIG. 4. Microwave power output as a function of wiggler length for constant wiggler field ($B_w = 4280$ G).

the effects of betatron motion on the parallel electron velocity.¹⁰ The electrons provide the source for the electromagnetic field.^{11,12} The source equation has been generalized in the simulations to include transverse variations of the electric field in the waveguide (the $TE_{n,1}$ modes, for n even, are followed). Neither the analytic theory nor the simulations account for space-charge forces, which we estimate to be a 10%–20% perturbation to the ponderomotive forces.

The gain curves derived from the numerical simulations are also shown in Figs. 3 and 4 along with the measurements. All but one important experimental parameter is known; the unknown parameter is the extent to which the electron beam is out of equilibrium (e.g., sausing) in the wiggler. A single value for the amplitude of the sausing oscillations is adequate both for the linear theory and for the numerical simulations to model correctly the observed exponential gain and saturated output power. With the exception of the $L_w = 1$ m gain curve, the predictions from both the simulation and the linear theory (exponential gain) agree both in shape and in amplitude to within 25% of the experimental results. In particular, the code correctly predicts the variation of microwave power with wiggler length beyond saturation (where the electrons have lost enough energy to shift to negative phase in the ponderomotive potential), and also the asymmetry in the 3-m gain curve. The discrepancy between the measured and calculated 1-m gain curves is probably a result of the small signal as well as the difficulty of the calculation of small extraction levels

nal. A special diagnostic probe was constructed to travel the length of the waveguide and provide real-time imaging of the electron beam position. The resolution of this probe is ± 0.5 cm. When this probe was inserted into the wiggler, the magnetron was replaced by a microwave attenuator and crystal detector (configuration A of Fig. 1) so that any amplified noise which was reflected off the moving probe could be detected. By measuring the microwave power as a function of probe position, we could determine the small-signal gain of the FEL.

Output power of the FEL amplifier was measured either by a vacuum laser calorimeter or calibrated crystal detectors preceded by approximately 100 dB of attenuation. When the calorimeter was used, the microwave pulse shape could be monitored with a crystal detector. All microwave elements (the magnetron and the calorimeter or output window) were transit-time isolated to prevent multiple passes of the microwave signal through the interaction region.

The signal gain in the super-radiant mode (no microwave input signal) was measured by means of the arrangement illustrated in configuration A of Fig. 1, and the results of this experiment are given in Fig. 2. The beam energy was 3.6 MeV ($\gamma=8.1$) and the wiggler magnetic field was 4.8 kG. The microwave radiation generated in the interaction region reflected off the face of the beam probe and was monitored by a crystal detector. Extracting the probe continuously lengthened the interaction region. The results (Fig. 2) indicate that the microwave signal grew at a rate of 13.4 dB/m for a beam current of 450 A.

We studied the amplifier gain by means of configuration B of Fig. 1 both as a function of wiggler magnetic field intensity and as a function of wiggler length. In this part of the experiment, the beam energy was 3.3 MeV. The dependence of the gain on wiggler field strength is shown in Fig. 3 for 1-, 2-, and 3-m-long, constant-amplitude wigglers. The peak output power of 80 MW achieved for both the 2- and 3-m-long wigglers indicates that the amplifier saturated near the 2-m point. The gain curves for the 1- and 2-m wigglers are relatively symmetric about the peak while the gain curve for the 3-m-long wiggler shows a marked asymmetry with a plateau on the long-wavelength side of the curve. This asymmetry is also shown in the simulations discussed below.

Near the magnetic field strength corresponding to the peak output of a 1-m-long wiggler, we examined the amplification as a function of wiggler length. The results of this experiment are shown in Fig. 4. It is clearly seen that the amplifier goes into saturation at 2.2 m; beyond this point, the amplified output power first decreases and then near 3 m starts to increase again. The gain as a function of wiggler length shows an exponential gain of approximately 15.6 dB/m up to

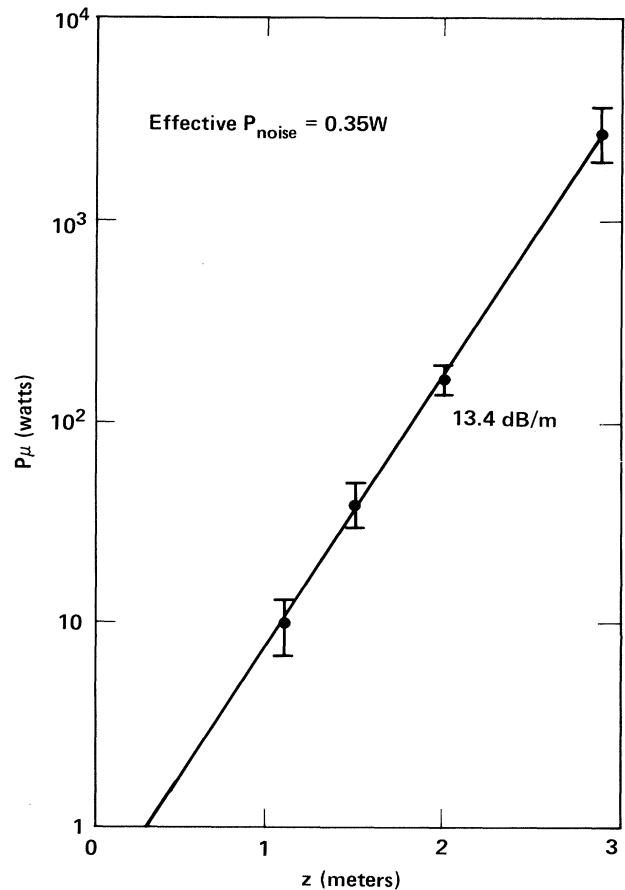


FIG. 2. Small-signal gain in the super-radiant mode as a function of wiggler length.

saturation ($L_w=2.2$ m). This is in close agreement with the small-signal gain measurement described above. (Note that the small-signal gain is proportional to $B_w/\gamma^{3/2}$, which is nearly the same in both cases.)

The linear theory best suited to the experiment has been derived by linearization of the single-particle, longitudinal (γ - ψ) equations of motion derived by Kroll, Morton, and Rosenbluth.⁸ The procedure is identical to that of Bonifacio, Pellegrini, and Narducci,⁹ with the addition of explicit betatron motion (i.e., emittance effects) and an integration over the waveguide. This version of the linear theory predicts a very steep dependence of gain on the electron beam emittance, and hence radius in the wiggler. The observed exponential gain, after we account for fractional coupling into the growing mode (launching losses), corresponds to a maximum beam radius of approximately 8 mm. This beam radius is consistent with the image seen on the axial probe.

The numerical simulations follow 4096 electrons in a single ponderomotive potential well.⁸ The particles undergo betatron oscillations in the transverse direc-

in the presence of numerical noise; the difference in peak powers is a discrepancy of only 10% in the exponential gain.

No self-consistent set of parameters explains both gain and efficiency in one-dimensional warm-beam models, when the emittance effects are approximated by an equivalent energy spread. We conclude that finite emittance cannot be represented as an equivalent energy spread.

We have successfully operated a FEL in the millimeter wave regime. This device, which has no axial magnetic field, is fully scalable to the visible wavelength regime. The results of linear theory and two-dimensional numerical modeling are in good agreement with the experimental results.

This work was performed jointly under the auspices of the U. S. Department of Energy by Lawrence Livermore National Laboratory, No. W-7405-ENG-48, and for the Department of Defense under the Defense Advanced Research Project Agency, ARPA Order No. 4856, Program Code No. 3B10, and was also supported in part by the Director, Advanced Energy Systems, Basic Energy Sciences, Office of Energy Research, U.S. Department of Energy, under Contract No. DE-AC03-76SF00098.

¹M. Billardon *et al.*, Phys. Rev. Lett. **51**, 1652 (1983).

²L. R. Elias *et al.*, Phys. Rev. Lett. **36**, 717 (1976).

³S. H. Gold *et al.*, Phys. Rev. Lett. **52**, 1218 (1984).

⁴J. A. Pasour, R. F. Lucey, and C. A. Kapetanacos, Phys. Rev. Lett. **53**, 1728 (1984).

⁵T. J. Orzechowski *et al.*, in *Free Electron Generators of Coherent Radiation*, edited by C. A. Brau, S. F. Jacobs, and M. O. Scully (SPIE, Bellingham, Wash., 1983), p. 65.

⁶T. J. Fessenden *et al.*, in *Proceedings of the Fourth International Topical Conference on High Power Electron and Ion Beam Research and Technology, Palaiseau, France, 1981*, edited by T. J. Fessenden *et al.* (Lawrence Livermore National Laboratory, Livermore, Cal., 1981), p. 813.

⁷Edge emittance is defined as the area in phase space which matches the acceptance of the emittance selector and contains 100% of the electron beam.

⁸N. M. Kroll, P. L. Morton, and M. R. Rosenbluth, IEEE J. Quantum Electron. **17**, 1436 (1981).

⁹R. Bonifacio, C. Pellegrini, and L. M. Narducci, Opt. Commun. **50**, 373 (1984).

¹⁰W. M. Fawley, D. Prosnitz, and E. T. Scharlemann, Phys. Rev. A **30**, 2472 (1984).

¹¹D. Prosnitz, A. Szoke, and V. K. Neil, Phys. Rev. A **24**, 1436 (1981).

¹²W. B. Colson, IEEE J. Quantum Electron. **17**, 1417 (1981).